Electronic structure and magnetization of $Zn_{1-x}Co_xO$ ternary alloys with zinc-blende, rocksalt and wurtzite phases

K. Souleh
Université Amar Telidji Laghouat: Universite Amar Telidji Laghouat
T. Smain
Universite Ziane Achour de Djelfa
H. Lidjici
Université Amar Telidji Laghouat: Universite Amar Telidji Laghouat
B. Lagoun
Université Amar Telidji Laghouat: Universite Amar Telidji Laghouat
M. Boucenna
Université de M'sila: Universite de M'sila
Nadir Bouarissa (n_bouarissa@yahoo.fr)
Universite de Msila

Research Article

Keywords: Electronic structure, Magnetism, Zn1-xCoxO alloys, ab initio calculations.

Posted Date: March 30th, 2021

DOI: https://doi.org/10.21203/rs.3.rs-344425/v1

Version of Record: A version of this preprint was published at Optical and Quantum Electronics on July 22nd, 2021. See the published version at https://doi.org/10.1007/s11082-021-02985-x.

Abstract

First-principles all electrons density-functional calculations for the band structure and magnetization of $Zn_{1-x}Co_xO$ ternary magnetic alloys, in three phases namely zinc-blende, rocksalt and wurtzite have been reported. The computations are spin-polarized. An inspection of our electronic properties showed that the alloy system of interest exhibits a semiconducting character where the nature of the gap depends on the considered phase. An analysis of electronic charge density suggests that the bonding has a partially covalent character for ZnO which becomes weaker as far as the Co concentration increases. CoO is found to reach a total magnetization of 3 μ_B per cell for zinc-blende and rocksalt phases and 6 μ_B per cell for wurtzite phase.

1. Introduction

Zinc-oxide (ZnO) is a II-VI semiconductor which is a promising material for device applications. This is because of its direct and wide band-gap energy and its high free-exciton binding energy [1–4]. On the other hand, cobalt oxide (CoO) is an inorganic compound which appears as olive-green to red crystals and has been used extensively in the ceramics and chemical industries and regarded as a novel, highly active heterogeneous catalyst for key processes in future energy and environmental technology [5, 6]. Alloys made for ZnO and CoO give $Zn_{1-x}Co_xO$ ternary alloys that are emerged as promising materials for different energy applications. As a matter of fact, the alloys under study offer a special interest in advanced spintronic devices. This is due to the fact that they may serve magnetism (spin) and semiconducting (charge) combined in one 'spintronic' device which makes it possible to exploit both charge and spin [7–13].

To take advantage of $Zn_{1-x}Co_xO$ ternary alloys one needs a thorough knowledge of their fundamental properties. These properties are essential for evaluating their expectable applications domain [14–21]. In fact, an accurate knowledge of the electronic properties of materials permits a precious information that may help in its synthesis and devices fabrication [22–25]. On the other hand, the knowledge of magnetic properties of materials plays an essential role in determining their suitability for a particular magnetic application [26–29]. Despite the importance of the fundamental properties of materials and the important technological applications of $Zn_{1-x}Co_xO$, the amount of available information on this material system is still limited, to the best of our knowledge. This has motivated us to do such an investigation of the electronic and magnetic properties of $Zn_{1-x}Co_xO$ ($0 \leq x \leq 1$) with hypothetical zinc-blende, rocksalt and wurtzite structures. The computations are carried out using the density-functional theory (DFT) calculations within the generalized gradient approximation (GGA). All calculations are spin-polarized. More details about computations are given in Sect. 2 of this paper.

2. Computational Details

The DFT has proven to be one of the most accurate theory for the calculation of the electronic structure of solids. The calculations are essentially based on the DFT [30, 31] using the full-potential linearized

augmented plane wave (FP-LAPW) method as implemented within the WIEN2K package [32]. All calculations are spin-polarized. The exchange-correlation terms are described using the GGA of Tran-Blaha modified Becke-Johnson (TB-mBJ-GGA) [33].

An elementary crystal structure containing atoms is established. During the relaxation, the atomic positions are allowed to relax within the cubic symmetry of space group.

In order to compute the material properties, we have used the DFT-based self-consistent cycle of the FP-LAPW method into WIEN2k code. This is surprisingly appropriate for the importance of band gap energies of solids when compared to the conventional GGA and gives accurate values of the band gap electronics which are close to the experimental ones.

We divided the region as interior non-overlapping space between muffin-tin spheres and the remaining as at an interstitial region between these spheres.

The space groups are: F4-3m (216), Fm3m (225) and P63mc (186) for zinc-blende, rocksalt and wurtzite structures, respectively. Each unit cell is divided into an interstitial region and non-overlapping muffin-tin (MT) spheres of radii R_{MT}.

For all structures zinc-blende, rocksalt and wurtzite, the R_{MT} is adopted to be 1.8 Bohr for Zn and Co atoms and 1.6 Bohr for O atoms. For all structures being considered here and for all concentrations of $Zn_{1-x}Co_xO$, we choose a grid of meshes for sampling the Brillouin zone using the Monkhorst and pack scheme [34, 35]. A plane wave cutoff of $R_{MT}k_{max} = 7$ is used for all structures of interest and for all concentrations of $Zn_{1-x}Co_xO$, where k_{max} is the magnitude of the largest k vector in the plane wave expansions. The alloy concentrations x of $Zn_{1-x}Co_xO$ have been considered from 0 to 1 with a step of 0.25. The alloyed structures have been completely optimized and the iteration process is repeated till the convergence of the total energy of the crystal of interest is ensured to less than 10^{-5} Ry.

3. Results And Discussion

The electronic band structures of $Zn_{1-x}Co_xO$ in hypothetical zinc-blende, rocksalt and wurtzite structures with various Co compositions x ($0 \leq x \leq 1$) have been computed in this work using the TB-mBJ-GGA approach. For magnetic alloys and CoO compound the spin direction is taken into consideration. Since the picture of band structures for various concentrations x is similar, we display only the electronic structure of the equimolar alloy $Zn_{0.50}Co_{0.50}O$ in the three structures being considered here and for both spin channels. Our results are shown in Fig. 1. We observe that qualitatively all bands for different structures of interest look like similar and resembles to those reported previously for other semiconducting materials [36–39]. Quantitatively, the main difference lies in the magnitudes of the band gap energies. A close inspection of these band structures indicates that for a spin up channel, $Zn_{0.50}Co_{0.50}O$ in its zinc-blende structure is a semiconductor material with a direct band gap ($\Gamma \rightarrow \Gamma$) of magnitude 2.04 eV, and in its rocksalt structure is a semiconductor material with an indirect band gap

(R→Γ) of magnitude of 1.12 eV, whereas in its wurtzite structure is a semiconductor material with a direct band gap (Γ→Γ) of magnitude of 2.094 eV.

The fundamental band gap energy (E_g) has been determined from the electronic band structures of $Zn_{1-x}Co_xO$ in the interval 0–1 for all structures being considered in this work. The evolution of E_g as a function of Co content for zinc-blende, rocksalt and wurtzite hypothetical structures of $Zn_{1-x}Co_xO$ is illustrated in Table 1 and Fig. 2. Note that for zinc-blende $Zn_{1-x}Co_xO$ as x increases, E_g decreases monotonously in a non-linear way. It shows a red shift from that of pure ZnO (x = 0) reaching about 1.07 eV for x = 1 (CoO). The same behavior of E_g versus x can be seen for rocksalt $Zn_{1-x}Co_xO$, where E_g decreases from 3.12 eV for ZnO to 1.06 eV for CoO, bearing in mind that the gap in this case is indirect. As far as wurtzite $Zn_{1-x}Co_xO$ is concerned, E_g varies non-monotonously and in a non-linear way. It is 2.86 eV for ZnO and 1.98 eV for CoO. The same trend of E_g versus x has been reported experimentally by Kim and Park [11] for $Zn_{1-x}Co_xO$ alloys using spectroscopic ellipsometry at room temperature.

Table 1
Evolution of the fundamental band-gap energy (Eg) as a function of Co content for zinc-blende, rocksalt and wurtzite hypothetical structures of $Zn1_{-x}Co_xO$.

N	E(Γ-Γ) (eV) Zinc-blende	E(R-Γ) (eV) Rocksalt	E(Γ-Γ) (eV) Wurtzite
0 (ZnO)	2.65	3.12	2.86 3.23 [40]; 2.77 [41]
0.25	2.28	1.6	2.35
0.50	2.04	1.12	2.09
0.75	1.93	1.1	1.85
1 (CoO)	1.57	1.06	1.98

Hence, for ZnO (x = 0), the type of the band-gap structure is a direct (Γ→Γ), whereas for other types (starting from x = 0.25 to x = 1) of band-gap structure, it is an indirect band-gap structure (R→Γ). On the other hand, the energy band-gap in ternary semiconductor alloys for $Zn_{1-x}Co_xO$ as a function of alloy composition x is decreased when going from 0 to 1, whereas the ternary alloy of interest becomes a R→Γ indirect band-gap structure once its x value becomes 0.25 and so over. We cite some references here [43–46] to compare with.

Our calculations have been done generally at a room temperature and ambient pressure. Remark that almost the same trend of Eg versus x was reported experimentally [11] for $Zn_{1-x}Co_xO$ alloys at a room temperature. The calculated value of E_g (2.856 eV) for wurtzite ZnO is slightly underestimated with

respect to that of experiment (3.23 eV) measured by Neogi et al. [40]. Nevertheless, this value looks closer to experiment than that of 2.77 eV reported very recently by Algarni et al. [41] using the same approach as that used here but differs in details (a grid of meshes is used here for sampling the Brillouin zone, whereas that used in Ref. [41] is meshes). The other E_gs are also expected to be underestimated with respect to experiment. This is generally a common trend known for DFT in the GGA computation of E_gs in semiconductors [42]. Hence, one may say that the types of the band gap structures are direct when their types of interest belongs to a direct ($\Gamma \rightarrow \Gamma$) transition (which corresponds to zinc-blende and wurtzite structures of $Zn_{1-x}Co_xO$ at ZnO (x = 0)) and are indirect ($R \rightarrow \Gamma$) when the types of band gap structures are indirect transition (which is the case for rocksalt $Zn_{1-x}Co_xO$ from x = 0.25 to x = 1).

The density of states (DOS) of $Zn_{1-x}Co_xO$ ($0 \leq x \leq 1$) has also been computed for zinc-blende, rocksalt and wurtzite structures so as to investigate the electrons distribution on various orbitals. Our results regarding DOS for ZnO, $Zn_{0.50}Co_{0.50}O$ and CoO are plotted in Fig. 3. A close examination of DOS for zinc-blende structure (Fig. 3(a)) indicates that the predominant contribution for the energy bands near the Fermi level of the crystal ZnO is that coming from the Zn-d electrons. The situation appears to be similar for rocksalt (Fig. 3(b)) and wurtzite (Fig. 3(c)) ZnO structures. Thus, the Zn-d electrons are important in the conductibility of ZnO for the three phases of interest. At these regions the DOS consists mainly of Zn-d and O-p states. The first region of DOS for wurtzite ZnO is the most tightly bound energy band. For Co-alloyed ZnO with x = 0.50, one can note that the dominant contributions are due to the d electrons of the Zn and Co atoms and the p electrons of the O atoms. This is true for all structures being considered in this work. As far as CoO is concerned, the dominant contributions come from the d electrons of the Co atoms and p electrons of the O atoms for zinc-blende, rocksalt and wurtzite structures. The 2p electrons of oxygen atoms contribute to the minimum of the conduction band. When going from ZnO to CoO, one can observe that the intensity of O-p orbitals in the conduction bands is reduced.

The study of the electronic charge densities in semiconducting materials is of fundamental interest. This is because it gives important information on the chemical bonding properties, interstitial impurities and response to perturbations in the materials under study [47–51]. In this respect, the valence electron charge densities for $Zn_{1-x}Co_xO$ ($0 \leq x \leq 1$) in zinc-blende, rocksalt and wurtzite structures are computed. In this work, we present in Fig. 4 the charge distributions in all structures of interest for Co compositions x = 0 (ZnO), x = 0.50 and x = 1 (CoO). As can be observed from the contour plots of Fig. 4, in ZnO (x = 0) most of the charges are located in the inter-atomic region and shifted towards the O anion. This is due to the fact that ZnO involves a charge transfer from the atoms II to the atoms VI indicating the ionic character of ZnO crystal. The bottom bands can be seen as s-like atomic orbitals. The middle gap of bands form the covalent bond. Practically, there is a total absence of charges in the interstitial regions. By alloying ZnO and CoO, for example $Zn_{0.50}Co_{0.50}O$ (Fig. 4(b)), the shift towards the anion becomes more important than in ZnO, suggesting that the bonding has a more ionic character than that of ZnO. When reaching CoO (x = 1) (Fig. 4c), the Co-O interaction seems to be purely ionic which is consistent with the experimental results of Jauch and Reehuis [52]. The general features of the electronic charge distribution

in zinc-blende structures seem to resemble to those in rocksalt structures but quite different in details from those of wurtzite structures.

The total magnetic moment of $Zn_{1-x}Co_xO$ has also been computed in the alloy composition interval 0–1 and for all structures being considered in this work. The evolution of the total magnetic moment as a function of Co content is shown in Fig. 5. This has been done for zinc-blende (Fig. 5(a)), rocksalt (Fig. 5(b)) and wurtzite (Fig. 5(c)) structures. Note that as the Co concentration is augmented from 0 to 1, the total magnetic moment of $Zn_{1-x}Co_xO$ increases for all structures of interest. The behavior of the total magnetic moment is monotonous and in a linear way. Interestingly, at the extreme case of CoO ($Zn_{1-x}Co_xO$, x = 1) the total magnetic moment is 3.0, 3.0 and 6.0 μ_B per cell for zinc-blende, rocksalt and wurtzite structures, respectively, whereas for the equimolar alloy $Zn_{0.50}Co_{0.50}$ O the total magnetic moment is calculated to be 1.50, 1.50 and 3.0 μ_B per cell for zinc-blende, rocksalt and wurtzite structures, respectively. The magnetic moment of Co^{2+} is associated to localized d electrons and the magnetic properties of CoO originate from the atomic magnetic moments of Co^{2+} ions.

4. Conclusions

The electronic band structure and magnetic properties of ZnO alloyed with CoO were studied. The computations were performed in the DFT framework using the FP-LAPW method. The exchange-correlation potential was described using the TB-mBJ-GGA approach. The hypothetical zinc-blende, rocksalt and wurtzite structures were considered for $Zn_{1-x}Co_xO$. The examination of the band structure and DOS showed that the alloy system under study exhibits a semiconducting character and that the nature of its gap depends on the considered phase. The bonding character of $Zn_{1-x}Co_xO$ was inspected and discussed via the electronic charge distributions. Our results showed that while a partially covalent character appears for ZnO, this covalent character becomes weaker as far as the Co content is increased increasing thus the ionicity character. The total magnetic moment was found to augment in a linear way with enhancing the alloy composition x from 0 to 1, reaching a value of 3.0 μ_B per cell for CoO in the zinc-blende and rocksalt structures and that of 6.0 μ_B per cell for CoO in the wurtzite structure. The present results may be useful for the spintronics applications.

References

[1] A. Janotti, C. G. Van de Walle, Rep. Prog. Phys. 72 (2009) 126501

[2] S. B. Ogale, Thin Films and Heterostructures for Oxide Electronics, New York, Springer, 2005

[3] C. Jagadish, S. J. Pearton, Zinc Oxide Bulk, Thin Films and Nanostructures, New York, Elsevier, 2006

[4] S. Saib, N. Bouarissa, Phys. Status Solidi B 244 (2007) 1063

[5] R. Kannan, M. S. Seehra, Phys. Rev. B 35 (1987) 6847

[6] P. S. Silinsky, M. S. Seehra, Phys. Rev. B 24 (1981) 419

[7] G. Amita, Novel room temperature ferromagnetic semiconductors, United States: N. P., 2004.Web.DOI:10.2172/878314

[8] M. Tortosa, M. Mollar, F. J. Manjón, B. Mari, J. F. Sánchez-Royo, Phys. Status Solidi C 5 (2008) 3358

[9] T. Dietl, H. Ohno, F. Matsukura, Phys. Rev. B 63 (2001) 195205

[10] A. Dinia, J. P. Ayoub, G. Schmerber, E. Beaurepaire, D. Muller, J. J. Grob, Phys. Lett. A 333 (2004) 152

[11] K. J. Kim, Y. R. Park, Appl. Phys. Lett. 81 (2002) 1420

[12] A. A. Lotin, O. A. Novodvorsky, V. V. Rylkov, D. A. Zuev, O. D. Khramova, M. A. Pankov, B. A. Aronzon, A. S. Semisalova, N. S. Perov, A. Lashkul, E. Lahderanta, V. Ya. Panchenko, Semiconductors 48 (2014) 538

[13] X. Deng, H. Tüysüz, ACS Catal. 4 (2014) 3701

[14] S. Saib, N. Bouarissa, P. Rodríguez-Hernández, A. Muñoz, Physica B 403 (2008) 4059

[15] S. Adachi, Properties of Group-IV, III-V, and II-VI Semiconductors, Wiley, Chichester, 2005 and references therein

[16] S. Daoud, N. Bioud, N. Bouarissa, Mater. Sci. Semicond. Process. 31 (2015) 124

[17] S. Adachi, Properties of Semiconductor Alloys: Group-IV, III-V and II-VI Semiconductors, John Wiley & Sons Ltd., Chichester, 2009 and references therein

[18] S. Saib, N. Bouarissa, P. Rodríguez-Hernández, A. Muñoz, Eur. Phys. J. B 73 (2010) 185

[19] I. Vurgaftman, J. R. Meyer, L. R. Ram-Mohan, J. Appl. Phys. 89 (2001) 5815 and references therein

[20] N. Bouarissa, Phys. Lett. A 245 (1998) 285

[21] L. Hannachi, N. Bouarissa, Physica B 404 (2009) 3650

[22] M. L. Cohen, J. R. Chelikowsky, Electronic Structure and Optical Properties of Semiconductors, Springer-Verlag, Berlin, 1989

[23] S. Saib, N. Bouarissa, J. Phys. Chem. Solid. 67 (2006) 1888

[24] R. M. Martin, Electronic Structure: Basic Theory and Practical Methods, Cambridge, University Press, 2004

[25] N. Bouarissa, J. Phys. Chem. Solid. 67 (2006) 1440

[26] H. Ohno, J. Magn. Magn. Mater. 200 (1999) 110

[27] N. Moulai, N. Bouarissa, B. Lagoun, D. Kendil, J. Supercond. Nov. Magn. 32 (2019) 1077

[28] A. Bouarissa, A. Layadi, H. Maghraoui-Meherzi, Appl. Phys. A 126 (2020) 93

[29] Y. Harrache, N. Bouarissa, Solid State Commun. 295 (2019) 26

[30] P. Hohenberg, W. Kohn, Phys. Rev. 136 (1964) B 864

[31] W. Kohn, L. S. Sham, Phys. Rev. 140 (1965) A1133

[32] P. Blaha, K. Schwarz, G. K. H. Madsen, D. Kvasnicka, J. Luitz, WIEN2K, An Augmented Plane Wave + Local Orbitals Program for Calculating Crystal Properties, edited by Karlheinz Schwarz, Techn. Universität, Wien, Austria, 2008, ISBN-3-9501031-1-2

[33] F. Tran, P. Blaha, Phys. Rev. Lett. 102 (2009) 226401

[34] H. J. Monkhorst, J. D. Pack, Phys. Rev. B 13 (1976) 5188

[35] J. D. Pack, H. J. Monkhorst, Phys. Rev. B 16 (1977) 1748

[36] S. Zerroug, F. Ali Sahraoui, N. Bouarissa, Appl. Phys. A 97 (2009) 345

[37] F. Benmakhlouf, A. Bechiri, N. Bouarissa, Solid State Electron. 47 (2003) 1335

[38] K. Kassali, N. Bouarissa, Microelectron. Eng. 54 (2000) 277

[39] N. Bouarissa, Phys. Status Solidi B 231 (2002) 391

[40] S. K. Neogi, R. Karnakar, A. K. Misra, A. Banerjee, D. Das, S. Bandyopodhyay, J. Magn. Magn. Mater. 346 (2013) 130

[41] H. Algarni, A. Gueddim, N. Bouarissa, M. A. Khan, H. Ziani, Res. Phys. 15 (2019) 102694

[42] S. Zerroug, F. Ali Sahraoui, N. Bouarissa, Eur. Phys. J. B 57 (2007) 9

[43] M. Othman, S. Salih, M. Sedighi, E. Kasap, Res. Phys. 14 (2019) 102400

[44] N. N. Jardow, M. S. Othman, N. F. Habubi, S. S. Chiad, K. A. Mishjil, I. A. Al-Baidhany, Mater. Res. Exp. 6 (2019) 116434

[45] M. SH. Othman, J. Modern Phys. 4 (2013) 185

[46] M. Sh. Othman, Aro-The Scientific J. Koya University 8 (2020) 29

[47] J. P. Walter, M. L. Cohen, Phys. Rev. Lett. 26 (1971) 17

[48] N. Bouarissa, Infrared Phys. Technol. 39 (1998) 265

[49] S. L. Richardson, M. L. Cohen, S. G. Louie, J. R. Chelikowsky, Phys. Rev. B 33 (1986) 1177

[50] N. Bouarissa, Mater. Chem. Phys. 65 (2000) 107

[51] N. Bouarissa, F. Annane, Mater. Sci. Eng. B 95 (2002) 100

[52] W. Jauch, M. Reehuis, Phys. Rev. B 65 (2002) 125111

Figures

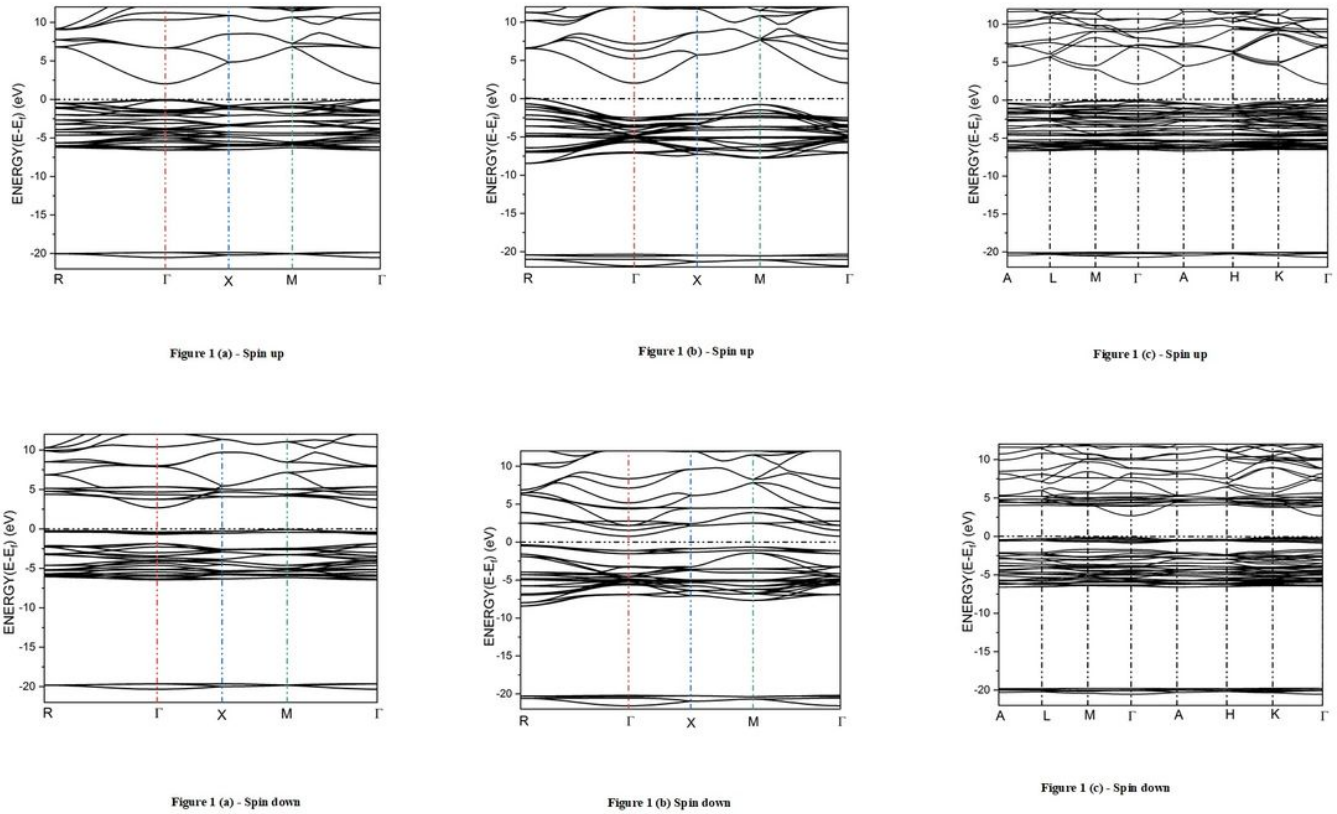

Figure 1

Electronic band structure for Zn0.50Co0.50O in (a) the zinc-blende structure (b) the rocksalt structure and (c) the wurtzite structure, considering both spin channels.

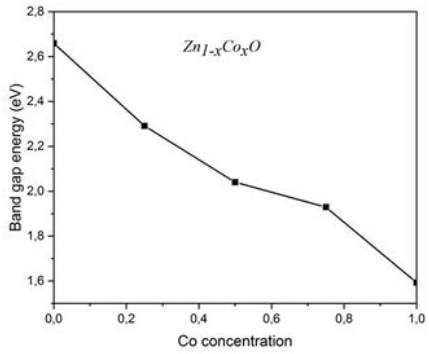

Figure 2 (a)

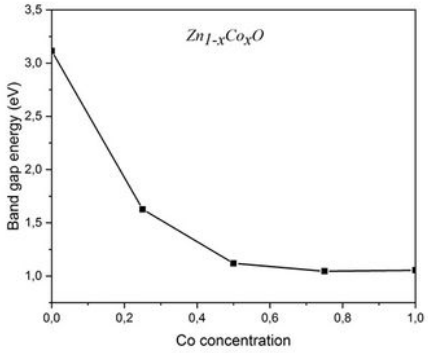

Figure 2 (b)

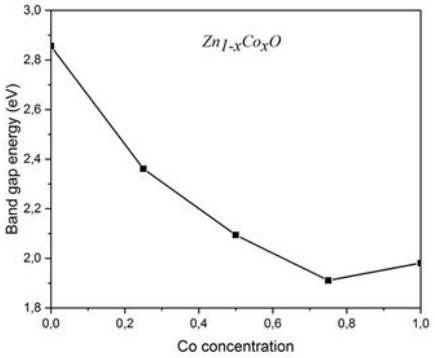

Figure 2 (c)

Figure 2

Fundamental band gap energy versus Co content in (a) the zinc-blende structure (b) the rocksalt structure and (c) the wurtzite structure for spin up channel.

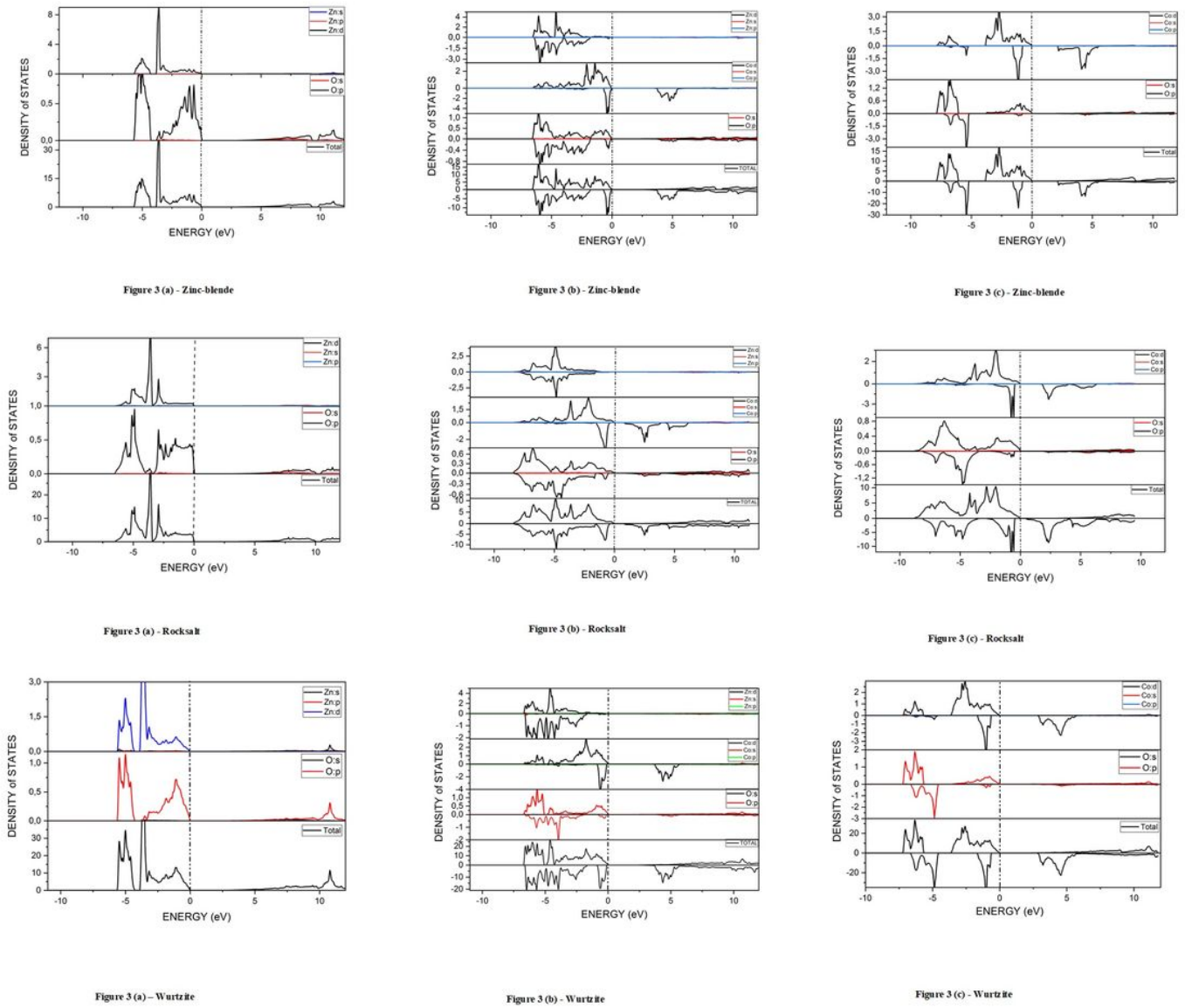

Figure 3 (a) - Zinc-blende

Figure 3 (b) - Zinc-blende

Figure 3 (c) - Zinc-blende

Figure 3 (a) - Rocksalt

Figure 3 (b) - Rocksalt

Figure 3 (c) - Rocksalt

Figure 3 (a) – Wurtzite

Figure 3 (b) - Wurtzite

Figure 3 (c) - Wurtzite

Figure 3

Density of states of (a) ZnO (b) Zn0.50Co0.50O and (c) CoO in the zinc-blende, rocksalt and wurtzite structures, considering both spin channels.

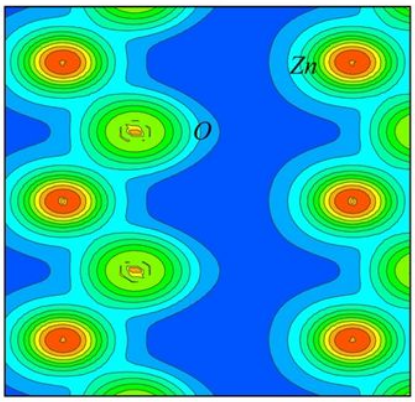

Figure 4 (a) - Zinc-blende

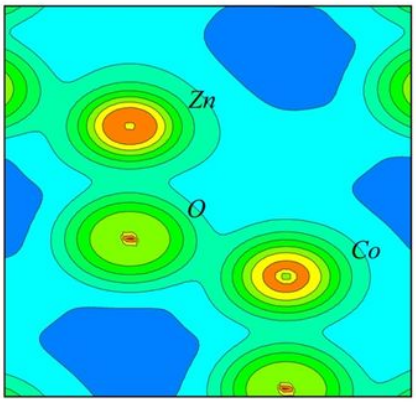

Figure 4 (b) - Zinc-blende

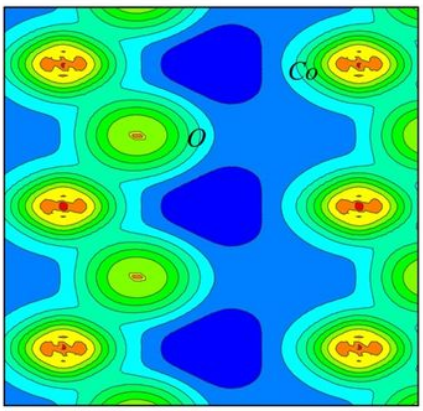

Figure 4 (c) - Zinc-blende

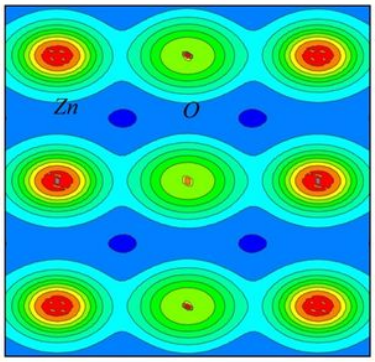

Figure 4 (a) - Rocksalt

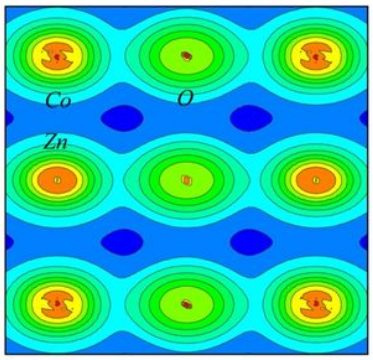

Figure 4 (b) - Rocksalt

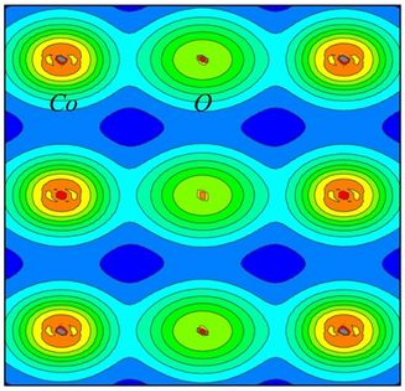

Figure 4 (c) -Rocksalt

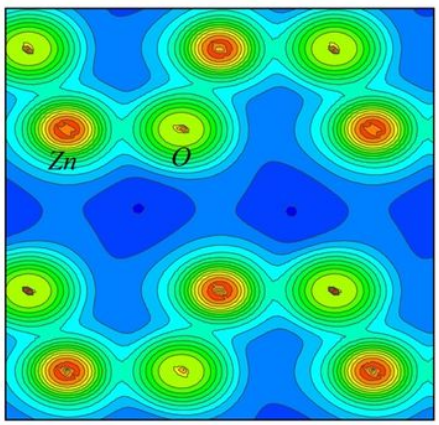

Figure 4 (a) - Wurtzite

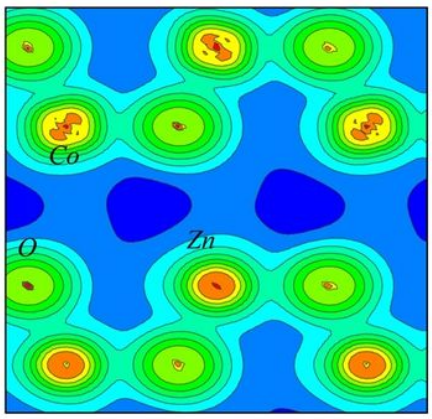

Figure 4 (b) - Wurtzite

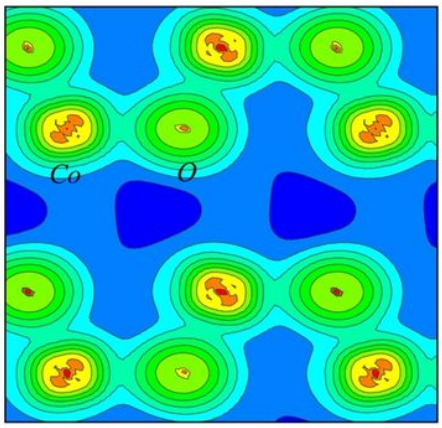

Figure 4 (c) - Wurtzite

Figure 4

Electronic valence charge density (contour plots) of (a) ZnO (b) Zn0.50Co0.50O and (c) CoO in the zinc-blende, rocksalt and wurtzite structures for spin up channel.

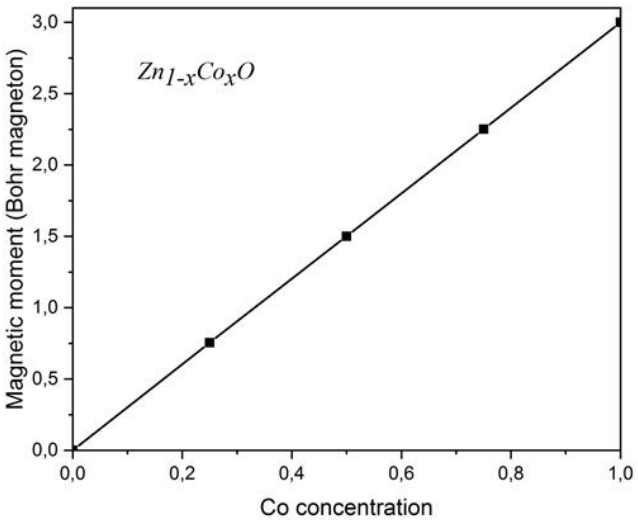

Figure 5 (a)

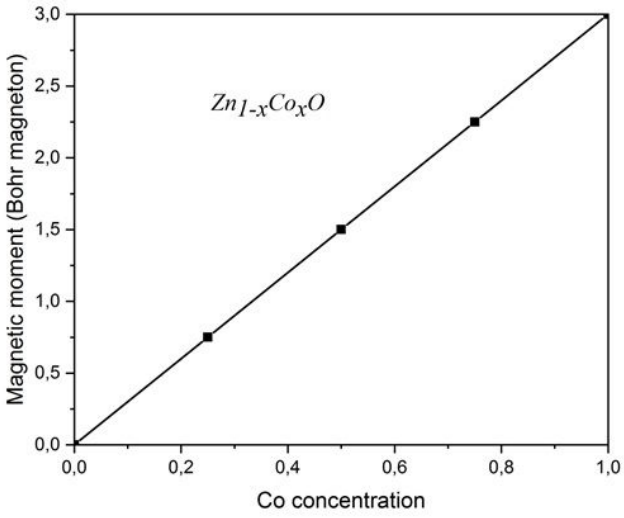

Figure 5 (b)

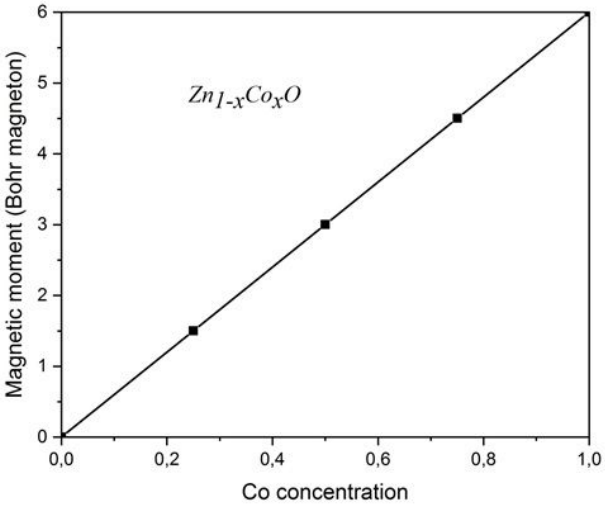

Figure 5 (c)

Figure 5

Total magnetic moment versus Co content in (a) zinc-blende structure (b) rocksalt structure and (c) wurtzite structure.